Predator-Prey Pigeon-Inspired Optimization for UAV ALS Longitudinal Parameters Tuning

HAIBIN DUAN, Senior Member, IEEE
MENGZHEN HUO
ZHIYUAN YANG
Beihang University (BUAA), Beijing, China

YUHUI SHI, Fellow, IEEE
Southern University of Science and Technology, Shenzhen, China

QINAN LUO
Beihang University (BUAA), Beijing, China

This paper presents a predator-prey pigeon-inspired optimization (PPPIO) algorithm for an automatic landing system of a fixed-wing unmanned aerial vehicle (UAV) in the longitudinal plane. A pitch command autopilot and two types of approach power compensators are presented and evaluated in automatic landing. The design of a glide slope command system and an approach power compensator are converted to a finite-dimensional optimization problem. The longitudinal flight controller parameters are optimized by the proposed PPPIO algorithm. The differences between the two proposed approach power compensators are also analyzed. The proposed optimization process can guarantee the control gains vector converge to an approximate optimal solution, and it is computationally much more efficient. Simulation results are presented to demonstrate that this approach helps solve control system optimization problems for different criteria and attains a rather accurate result. As verified by these simulation results, the proposed automatic landing system can help improve UAV's performance during the landing phase.

Manuscript received February 5, 2018; revised August 3, 2018; released for publication November 24, 2018. Date of publication December 13, 2018; date of current version October 10, 2019.

DOI. No. 10.1109/TAES.2018.2886612

Refereeing of this contribution was handled by I. Hwang.

This work was supported in part by the National Natural Science Foundation of China (NSFC) under Grant 61761136008, Grant 61761136008, Grant 91648205, and Grant 61333004, in part by the Aeronautical Foundation of China under Grant 2015ZA51013, and in part by the Science and Technology Innovation Committee Foundation of Shenzhen under Grant ZDSYS201703031748284.

Authors' addresses: H. Duan, M. Huo, Z. Yang, and Q. Luo are with the State Key Laboratory of Virtual Reality Technology on Systems, School of Automation Science and Electrical Engineering, Beihang University (BUAA), Beijing 100083, China, E-mail: (hbduan@buaa.edu.cn; mzhuo@buaa.edu.cn; yangzhiyuan@buaa.edu.cn; inanluo@buaa.edu.cn); Y. Shi is with the Shenzhen Key Laboratory of Computational Intelligence, Department of Computer Science and Engineering, Southern University of Science and Technology, Shenzhen 518055, China, E-mail: (shiyh@sustc.edu.cn). *(Corresponding author: Haibin Duan.)*

I. INTRODUCTION

Unmanned aerial vehicle (UAV) is becoming an integral part of future military forces and will be used for complex tasks including surveillance, reconnaissance, precision strike, and aerial refueling missions. Therefore, more attention is now paid to various control problems associated with UAV. The landing of UAV is one of the most difficult operations in regard to accuracy and safety, and it is a harder task for an UAV with a lower aerodynamic stability [1], [2]. Therefore, the automatic landing of UAV is an important and valuable research. The wind disturbances arouse flight path tracking errors related to air disturbance along the approach path, while the random wind turbulence causes the perturbation of the aircraft and reduces its landing accuracy. Then, the automatic landing system (ALS) for a fully automatic approach and landing of UAV have been developed to solve the automatic landing problems [3]. In order to overcome the difficulties and expand the operational envelope of the UAV, there has been a lot of studies and development in the area of automatic landing [4]. The robust and sliding mode control theory has been utilized to solve linear and nonlinear automatic landing control problems and its invariance of quasi-sliding mode manifests ideal robustness [5]. The Robust technique is also employed to eliminate the influence of uncertainties and disturbances [6].

The objective of the ALS design provides a precise automatic control process for the UAV approaching and landing [7]. Most of the improvements in the ALS are about the guidance instruments [8], [9]. However, very few literatures focus on the design of the approach power compensator (APC). Since neither the thrust nor the elevator can control the altitude directly, ALS is required to achieve flight approach control by coupling various commands to the aircraft autopilot and together with an APC [10]. The autopilot and the APC contain feedback gains from pitch rare, normal accelerometer, elevator deflection, airspeed and angle of attack (AOA). These feedback signals modulate the elevator and the engine thrust to maintain a desired airspeed or attack angle. Then, the autopilot and APC are integrated to keep the flight path angle at the reference value. This close-loop system improves the landing ability by approximately decoupling the pitch control and thrust control [11].

Control parameters tuning in the ALS design is a complicated problem, which can be converted to a finite-dimensional optimization problem subject to aircraft performance constraints. For this optimization problem, cost functions are designed considering the airspeed response, pitch angle response, and attack angle response, together with some dynamic constraints. Therefore, the values of the control variables in the dynamic system have to be determined to obtain an approximate optimal performance.

Although the optimization problem can be solved based on optimal control theory and various numerical optimization techniques, the amount of computation may grow to an impractical level when the solution space increases. Furthermore, the convergence speed of optimal control-based algorithms depends heavily on the initial guess of the system states and control variables. Moreover, a large amount of analysis work should be previously done to deal with the system dynamics and control constraints [12]. Thus, using heuristic algorithms to solve the control parameters optimization problem has become a promising trend. Several heuristic optimization methods, such as genetic algorithm (GA), particle swarm optimization, simulated annealing, tabu search, etc., have been presented in the past decades [13]–[18]. These methods have been proved to be feasible, reliable, and effective ways to solve engineering problems encountered in many transportation systems, such as ground mobile robot, underwater vehicle, UAV, and aircrafts [19]–[21]. The main advantage of heuristic methods is that they do not need an explicit expression for the complicated nonlinear dynamics.

Recently, lots of evolutionary computation methods have been studied for scientific research and engineering applications [22]. Swarm algorithms have been applied to controller parameter optimization in many research works. Identifying controller parameters based on bio-inspired computing methods become a special hot topic. Li *et al.* [23] utilized GA to optimize the fixed control parameters of the flight control systems. Meng *et al.* [24] presented a hierarchical optimization model for self-reconfiguration of modular robots in changing environments. Recently, many optimal control-based algorithms and convexification-based techniques are adopted in numerous optimization problems, such as a space maneuver vehicle is optimized by a hybrid optimal control solver [25], time-optimal trajectories are generated rapidly by the convex optimization [26], aeroassisted vehicle trajectory optimization problems are solved by the improved gradient-based algorithm [27]. This paper focuses on the longitudinal ALS optimization based on predator-prey pigeon-inspired optimization (PPPIO) [28]. The ALS design is modeled as a parameter optimization problem with dynamical and algebraic constraints. For this reason, artificial intelligence algorithms and/or other optimization methods can be utilized to find the optimal solution. The ability of function optimization makes PPPIO effective for adjusting controller gains. The robustness of the controller is obtained by choosing optimal control gains that allow a wide range of disturbances to the controller.

This paper is organized as follows. In Section II, the UAV's aerodynamic is introduced. In Section III, the ALS consists of a longitudinal autopilot and two types of APCs are displayed, and PPPIO is presented to solve the parameter optimization problem. The APCs adopted in the ALS are also analyzed in Section III. Afterward, the validity of the proposed methodology is tested in various experiments to demonstrate its advantages in Section IV. Conclusions are presented in Section V.

II. PROBLEM FORMULATION

A. UAV Dynamics

Adopting assumptions including the local flatness of the earth, constant aircraft mass, and the earth reference frame being an inertial frame, the UAV nonlinear equations of 6 degree of freedom (DOF) can be deduced by the aerodynamic and kinematical equations as follows [29]:

$$\begin{aligned}\dot{V} = &\frac{1}{m}(P_x\cos\alpha\cos\beta - P_y\sin\alpha\cos\beta \\ &+ P_z\sin\beta + Z\sin\beta - Q) \\ &- g(\cos\alpha\cos\beta\sin\vartheta \\ &- \sin\alpha\cos\beta\cos\vartheta\cos\gamma \\ &- \sin\beta\cos\vartheta\sin\gamma \end{aligned} \tag{1}$$

$$\begin{aligned}\dot{\alpha} = &-\frac{1}{mV\cos\beta}\left(P_x\sin\alpha + P_y\cos\alpha + Y\right) \\ &+ \omega_z - \tan\beta\left(\omega_x\cos\alpha - \omega_y\sin\alpha\right)\frac{\delta y}{\delta x} \\ &+ \frac{g}{V\cos\beta}(\sin\alpha\sin\vartheta + \cos\alpha\cos\vartheta\cos\gamma) \end{aligned} \tag{2}$$

$$\begin{aligned}\dot{\beta} = &\frac{1}{mV}(-P_x\cos\alpha\sin\beta + P_y\sin\alpha\sin\beta \\ &+ P_z\cos\beta + Z) + \omega_x\sin\alpha + \omega_y\cos\alpha \\ &+ \frac{g}{V}(\cos\alpha\sin\beta\sin\vartheta - \sin\alpha\sin\beta\cos\vartheta\cos\gamma \\ &+ \cos\beta\sin\gamma\cos\vartheta) \end{aligned} \tag{3}$$

where V represents the airspeed of the UAV, Q represents the dynamic pressure of the UAV, m is the mass of UAV, α is the attack angle, β is the sideslip angle, ϑ is the pitch angle, and γ is the roll angle. P_x, P_y, and P_z denote three forces in the body axis which are generated by the thrust vector, X, Y, Z are the aerodynamic forces related to the body axis. ω_x, ω_y, ω_z denote the coordinate components of palstance, which can be expressed as

$$\begin{aligned}\dot{\omega}_x = &b_{11}\omega_y\omega_z + b_{12}\omega_x\omega_z \\ &+ \frac{I_y\left(M_x + M_{px}\right) + I_{xy}\left(M_y + M_{py}\right)}{I_xI_y - {I_{xy}}^2} \end{aligned} \tag{4}$$

$$\begin{aligned}\dot{\omega}_y = &b_{21}\omega_y\omega_z + b_{22}\omega_x\omega_z \\ &+ \frac{I_{xy}\left(M_x + M_{px}\right) + I_x\left(M_y + M_{py}\right)}{I_xI_y - {I_{xy}}^2} \end{aligned} \tag{5}$$

$$\dot{\omega}_z = \frac{I_x - I_y}{I_z}\omega_x\omega_y + \frac{I_{xy}}{I_z}\left({\omega_x}^2 - {\omega_y}^2\right) + \frac{\left(M_z + M_{pz}\right)}{I_z} \tag{6}$$

$$b_{11} = \frac{{I_y}^2 - I_yI_z - {I_{xy}}^2}{I_xI_y - {I_{xy}}^2} \tag{7}$$

$$b_{22} = \frac{I_xI_z - {I_x}^2 - {I_{xy}}^2}{I_xI_y - {I_{xy}}^2} \tag{8}$$

$$b_{12} = \frac{I_{xy}\left(I_z - I_y - I_x\right)}{I_xI_y - {I_{xy}}^2} \tag{9}$$

$$b_{21} = \frac{I_{xy}\left(I_y - I_z - I_x\right)}{I_xI_y - {I_{xy}}^2} \tag{10}$$

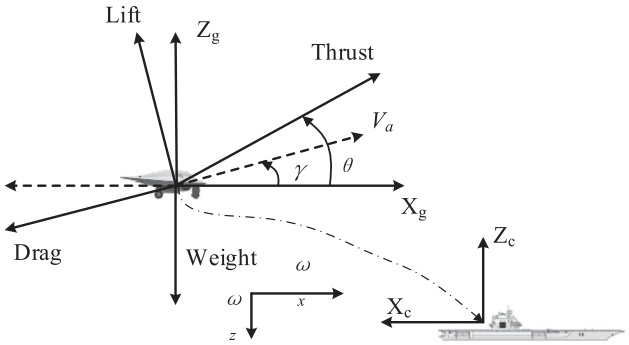

Fig. 1. UAV longitudinal dynamics.

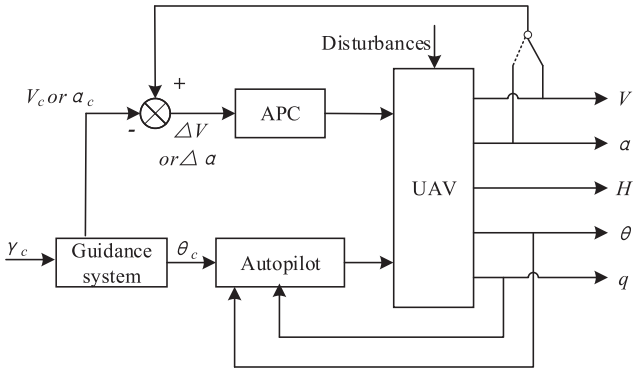

Fig. 2. Proposed longitudinal automatic landing control structure.

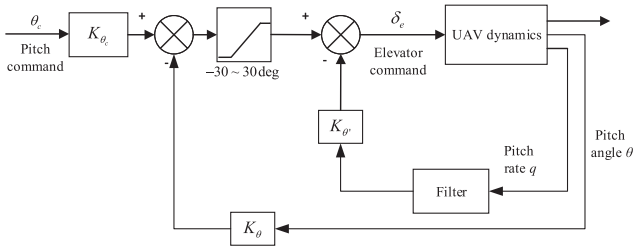

Fig. 3. Pitch command autopilot.

where I_x, I_y, I_z and M_x, M_y, M_z denote the coordinate components of inertia moment and resultant moment, respectively. In the body axis, we have

$$\dot{\gamma} = \omega_x - \tan\vartheta\left(\omega_y \cos\gamma - \omega_z \sin\gamma\right) \tag{11}$$

$$\dot{\vartheta} = \omega_y \sin\gamma + \omega_z \cos\gamma \tag{12}$$

$$\dot{\psi} = \frac{1}{\cos\vartheta}\left(\omega_y \cos\gamma - \omega_z \sin\gamma\right) \tag{13}$$

where ψ is the drift angle. Aerodynamic equations can be described as $Y = C_y qS$, $C_y = C_y(\alpha, \delta_z)$, $Z = \sum C_z qS$, $\sum C_z = C_z(\alpha, \delta_x) + C_z(\alpha, \delta_y)$, $Q = C_x qS$, $C_x = C_x(\alpha, \delta_z)$. δ_x, δ_y, δ_z are the coordinate components of deflection angles of the controlling surface. Aerodynamic moments can be described as

$$M_x = \sum m_x qsl, \sum m_x = m_x{}^{\beta}\beta + m_x(\alpha, \delta_x) + m_x\left(\alpha, \delta_y\right) + m_x{}^{\omega x}\omega_x\frac{l}{2V} + m_x{}^{\omega y}\omega_y\frac{l}{2V} \tag{14}$$

$$M_y = \sum m_y qsl, \sum m_y = m_y{}^{\beta}\beta + m_y(\alpha, \delta_x) + m_y\left(\alpha, \delta_y\right) + m_y{}^{\omega x}\omega_x\frac{l}{2V} + m_y{}^{\omega y}\omega_y\frac{l}{2V} \tag{15}$$

$$M_z = \sum m_z qsb_A, \sum m_z = m_z(\alpha, \delta_z) + m_z{}^{\omega z}\omega_z\frac{b_A}{V} + m_z{}^{\dot{\alpha}}\dot{\alpha}\frac{b_A}{V} \tag{16}$$

when the height and Mach are a constant value, aerodynamic coefficients $C_y(\alpha, \delta_z)$, $C_x(\alpha, \delta_z)$, $C_z(\alpha, \delta_x)$, $C_z(\alpha, \delta_y)$, $m_x(\alpha, \delta_x)$, $m_x(\alpha, \delta_y)$, $m_y(\alpha, \delta_x)$, $m_y(\alpha, \delta_y)$, $m_z(\alpha, \delta_z)$ are functions of the height, Mach, attack angle, and control surface. Aerodynamic derivatives $m_z{}^{\omega z}$, $m_z{}^{\dot{\alpha}}$, $m_x{}^{\beta}$, $m_x{}^{\omega x}$, $m_x{}^{\omega y}$, $m_y{}^{\beta}$, $m_y{}^{\omega x}$, $m_y{}^{\omega y}$ are specified values.

In most cases, the UAV maintains a nonsideslip flight. By controlling a sideslip angle and other lateral variables in 6-DOF equations to zeros automatically, we can focus on the longitudinal thrust controller optimization. The longitudinal state variables of UAV are referenced with respect to the earth reference frame, as shown in Fig. 1.

B. ALS Design

In this section, an ALS is designed to perform the UAV tracking a desired flight path angle during an approach. The block diagram of the proposed ALS for longitudinal flight control is shown in Fig. 2, including a pitch angle referenced autopilot and two types of APCs (airspeed or AOA referenced). The desired pitch angle is transformed into an attitude angle (pitch angle and AOA) and airspeed commands by a guidance system. The fixed-structure ALS design procedure is formulated as an optimization problem of control parameters and solved by employing the PPPIO method. This SI-based algorithm provides a reasonable solution of the ALS to the automatic landing process.

The ALS longitudinal autopilot can be considered as an inner loop control law configuration that should be specifically designed with rapid response capability to track the pitch angle command. As demonstrated in [5], the pitch angle is commonly controlled by an autopilot, as shown in Fig. 3, which uses the same components as the control augmentation system. This longitudinal autopilot is designed to provide continuous elevator commands δ_e, which makes the pitch angle track the desired pitch angle. Based on the longitudinal flight dynamic and the feedback technology, the pitch rate and the pitch angle are chosen as feedback variables to achieve significantly better damping and dynamic performance. In particular, a pitch command θ_c is first introduced into the closed-loop system, then, a pitch angle error signal, which represents the difference between the measured pitch angle and the command is calculated as the input of the controller. A pitch rate feedback q is integrated into the pitch angle signal to form an elevator command.

The dynamic response characteristics of the closed-loop system mainly depend on the feedback gains. The pitch rate filter and command limiter are also integrated, in which the filter values are adjusted to reduce impulse noises, and the limiter values are selected to permit satisfactory control

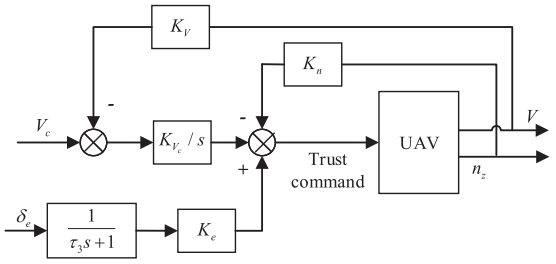

Fig. 4. Architecture of the airspeed referenced APC.

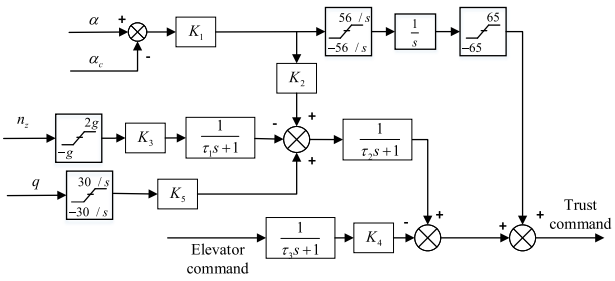

Fig. 5. Architecture of the AOA referenced APC.

inputs in the presence of large signals. Moreover, the inner loop should have higher gain amplitude in a low frequency range, which can be achieved by adopting a lag-lead filter on the pitch rate feedback signal [30].

The control system aims to make the system sufficiently stable when keeping a steady-state pitch angle under a determined command. Therefore, in the longitudinal pitch command autopilot, there are three main parameters K_{θ_c}, K_θ, and $K_{\theta'}$ to be adjusted, which can be considered as a pitch angle referenced proportional-integral-derivative (PID) controller tuning process. The control law of the pitch command autopilot [30] is expressed as

$$\delta_e = K_{\theta_c}\theta_c - K_\theta\theta - K_{\theta'}q. \tag{17}$$

The longitudinal autopilot achieves the commanded pitch angle, while the flight path angle must be controlled to land the UAV. This objective can be accomplished by using an APC, which is proposed for the purpose of relieving the pilot of the throttle management during approach [31], and is required to control the airspeed and AOA for pilot control inputs and external disturbance. The commonly used APCs include the system with constant airspeed and the system with constant AOA. Previous studies have demonstrated that the path angle can track a desired value accurately under the control of both these two types of APCs. In this paper, the APC automatically adjusts throttles to maintain the airspeed or AOA, and thus, combined the action of autopilot; the flight path angle can be maintained during an UAV landing approach.

To hold fixed airspeed or AOA, the APC should rapidly reduce the error in acquiring the glide path. Thus, as in the case of flight path control, it is difficult to guarantee the characteristics. Moreover, significant closed-loop response and stability imply that APC should have different effective orders and damping in different frequency. Thus, it is quite hard to select optimum APC gains for ALS performance objectives that provide the superior integrated system response.

The influence of wind disturbances on ALS flight path control also results in airspeed changes. These changes are important to the approach task. The airspeed referenced APC is applied to maintain a constant airspeed. The block diagram of the proposed airspeed referenced APC is shown in Fig. 4. The basic relations expressed by this diagram involve the feedback of airspeed V, normal acceleration n_z, and elevator defection δ_e. The airspeed feedback signal is employed to track a desired airspeed V_c, and the normal acceleration is used to increase the damping coefficient of the system. In the design of airspeed referenced APC, there are four parameters K_V, K_{V_c}, K_n, and K_e that need to be determined. The control law of airspeed referenced APC [32] is given by

$$\delta_T = (V_c - K_V V)\frac{K_{V_c}}{s} - K_n n_z + \frac{K_e}{\tau_3 s+1}\delta_e. \tag{18}$$

The other method of achieving a desired flight path angle is to control the AOA to a reference value, since the flight path angle represents the difference between the pitch angle and AOA. This is accomplished by using an AOA referenced APC. The block diagram of the proposed AOA referenced APC is shown in Fig. 5. The AOA referenced control law design is consist of the following input terms: AOA for the primary feedback, integral AOA signal to eliminate biases and track the steady-state reference value, normal acceleration n_z to augment the flight path damping, elevator/stabilizer position δ_e, and pitch rate q to provide a lead term for UAV pitch maneuvers. The AOA error signal (the difference between the measured value and the desired value) is sent to the system, which develops thrust commands for the UAV. Variations in vertical normal acceleration are adopted to minimize the effects of wind disturbances. Data from the pitch rate transducer and the stick/stabilizer position are also integrated to control an electromechanical servo actuator, which is coupled to the throttle setting of the engine. Parameters τ_1, τ_2, and τ_3 are coefficients of sensors corresponding to the AOA, the normal acceleration, and the elevator deflection, respectively. In the design of AOA referenced APC, there are five parameters K_1, K_2, K_3, K_4, and K_5 to be determined, which correspond to AOA gains and damping coefficients. The control law of AOA referenced APC [32] is presented as

$$\delta_T = \left[(\alpha-\alpha_c)K_1K_2 - \frac{K_3}{\tau_1 s+1}n_z + K_5 q\right]\frac{1}{\tau_2 s+1} + \frac{(\alpha-\alpha_c)K_1}{s} - \frac{K_4}{\tau_3 s+1}\delta_e. \tag{19}$$

III. PPPIO METHOD APPLIED TO ALS PARAMETERS OPTIMIZATION

Pigeon-inspired optimization (PIO) [15] is a novel evolutionary computation algorithm that simulates the

mechanisms of homing pigeons. Map- and compass-like information are used at the beginning of their journey, home and landmarks provide more information in the midway. During their journey, their route is revised timely to guarantee that they can reach the destination through the optimal one. Therefore, there are two operators in the PIO algorithm, i.e., the map and compass operator and the landmark operator. The destination of the journey is simulated as the optimal solution of the problem and the position of each pigeon is a feasible solution. The algorithm has been widely improved and applied to optimization problems in many fields since it was proposed, such as electromagnetic field [33], neural network [16], air combat [15], UAVs swarm formation [34], etc.

The function of the magnetic field and the Sun are simulated in PIO, which is named the map and compass operator. In this operator, the position X_i and velocity V_i of pigeon i in the tth iteration is presented as

$$V_i(t) = V_i(t-1) \cdot e^{-Rt} + \text{rand} \cdot (X_g - X_i(t-1)) \quad (20)$$

$$X_i(t) = X_i(t-1) + V_i(t) \quad (21)$$

where R is the map and compass factor, which can be adjusted according to the problem. rand is a random number between 0 and 1. X_g is the global best position in current iteration.

The landmark operator is designed in PIO to simulate the function of regular landmarks. Pigeon in the best position in the current iteration is considered as the intermediate destination. Half of the pigeons that are far from the intermediate destination are ignored in the landmark operator. The number of pigeons in the tth iteration is defined as follows:

$$N_P(t) = \text{ceil}\left(\frac{N_P(t-1)}{2}\right). \quad (22)$$

The center position of pigeons at the tth iteration is defined as

$$X_c(t) = \frac{\sum X_i(t) \cdot \text{fitness}\,(X_i(t))}{N_P \sum \text{fitness}\,(X_i(t))} \quad (23)$$

where fitness $(\cdot)$ is the criterion to evaluate the quality of each pigeon individual. It is defined as $\text{fitness}\,(X_i(t)) = \frac{1}{f_{\min}(X_i(t))+\varepsilon}$ for minimum optimization problems or $\text{fitness}(X_i(t)) = f_{\max}(X_i(t))$ for maximum optimization problems.

The predator-prey mechanism is simulated in this paper to increase the diversity of the pigeon and overcome the problem of local optimum traps. Predators hunt prey and the preys need to try their best to run away from predators in the predatory behavior in nature. PIO improved with the predator-prey mechanism is named PPPIO in this study. The predator is selected according to the worst solution, which is defined as follows:

$$S_{\text{predator}} = S_{\text{worst}} + \rho(1 - t/t_{\max}) \quad (24)$$

where S_{predator} a predator and S_{worst} is the worst solution. t is the number of current iteration, and $t_{\max}$ is the number of the total iterations. ρ is the hunting rate and it can be adjusted.

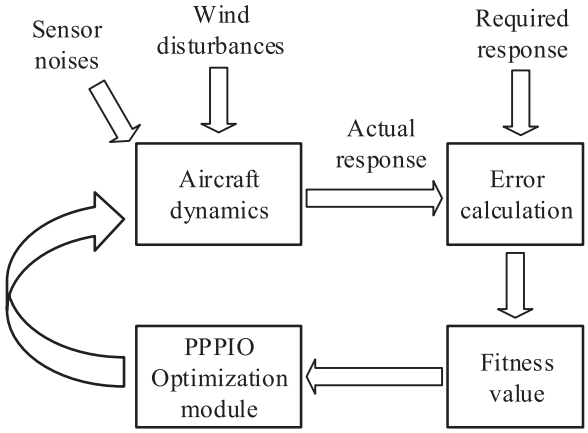

Fig. 6. Control parameters optimization process based on PPPIO.

The prey fleeing and provides the solutions to maintain a distance from the predator, namely keep away from the worst solution, which is defined as follows:

$$\begin{cases} S_{t+1} = S_t + \rho e^{-|d|}, d > 0 \\ S_{t+1} = S_t - \rho e^{-|d|}, d < 0 \end{cases} \quad (25)$$

where d is the distance between the solution and the predator.

The control law design aims to optimize the longitudinal autopilot and APC control gain terms to minimize flight path deviations in the presence of wind disturbance. In the design of previously demonstrated ALS, there are two sets of parameter vectors $[K_{\theta_c}, K_\theta, K_{\theta'}, K_V, K_{V_c}, K_n, K_e]$ and $[K_{\theta_c}, K_\theta, K_{\theta'}, K_1, K_2, K_3, K_4, K_5]$ related to different types of APCs, which corresponds to airspeed or AOA control gains and other damping coefficients. The pigeons in the PPPIO are set to be these two types of parameter vectors. The range for each parameter is defined according to the control structure.

For utilizing the PPPIO algorithm to optimize parameter combinations for the ALS, the fitness function is given as follows:

$$J = \int_0^{T_t} t\,|\varepsilon(t)|\,\text{dt} \quad (26)$$

where $\varepsilon(t) = (\theta(t) - \theta_c) + w_1(\alpha(t) - \alpha_c) + w_2(V(t) - V_c)$ represents the error between pitch angle, airspeed or AOA actual outputs and referenced signals. In airspeed referenced APC, the weight coefficients w_1 and w_2 are defined as 0 and 1, respectively. On the contrary, the weight coefficients are prescribed as 1 and 0 in an AOA referenced APC.

First, the population of PPPIO is defined. Then, the optimization process based on PPPIO is illustrated in Fig. 6. Actual responses of the UAV are obtained by the calculation of the motion equations, including the actuator and engine dynamics, wind disturbances and sensor noises. The fitness value of each pigeon is computed by comparing the actual response and the required response. Finally, if the termination conditions (maximum number of iterations is

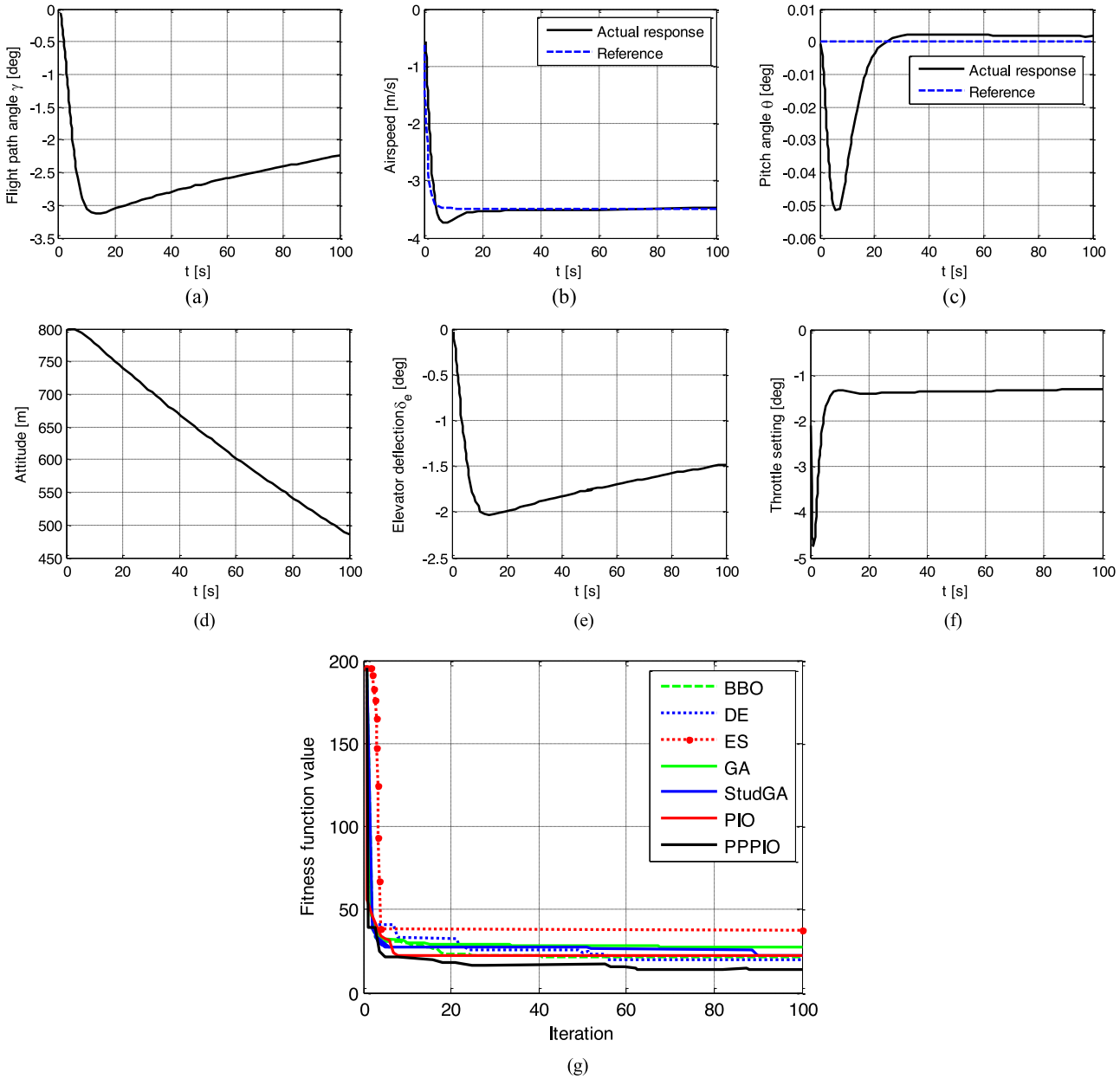

Fig. 7. Flight path angle tracking performance by airspeed referenced APC in no-wind condition. (a) Flight path angle response. (b) Airspeed response. (c) Pitch angle response. (d) Altitude response. (e) Elevator deflection. (f) Throttle setting. (g) Comparison evolution cures of PPPIO and other algorithms for airspeed referenced ALCS optimization.

reached or the relative error is lower than an expected value) are satisfied, then it results in the optimal parameters and optimal cost value. Otherwise, continue the optimization process.

The computational costs of basic PIO and PPPIO algorithm could be easily obtained by the mathematical expressions. The population size of the pigeons is defined as N_P, the dimension of the parameter vectors is defined as D. Additionally, the computational cost of objective function J is L_f. The complexity of the map and compass operator in basic PIO algorithm can be described as $O(N_P(D + L_f))$. Likewise, the complexity of the landmark operator could be obtained as $O(N_P \log N_P + D \log N_P + L_f \log N_P)$. Define the total iteration as N_c, then we can obtain the computational cost of basic PIO as $O(N_c(N_P \log N_P + DN_P + L_f N_P))$ [35].

In our proposed PPPIO algorithm, the computational cost of predator-prey mechanism is L_{PP}. Since the revised map and compass operator is designed more sophisticated to increase the diversity of the pigeon and overcome the problem of local optimum traps, the computational cost increases as $O(N_P(D + L_f + L_{PP}))$. The computational cost of a landmark operator in PPPIO algorithm is the same as that in PIO algorithm. Therefore, the total computation cost of PPPIO algorithm is $O(N_c(N_P \log N_P + DN_P + L_f N_P + L_{PP} N_P))$.

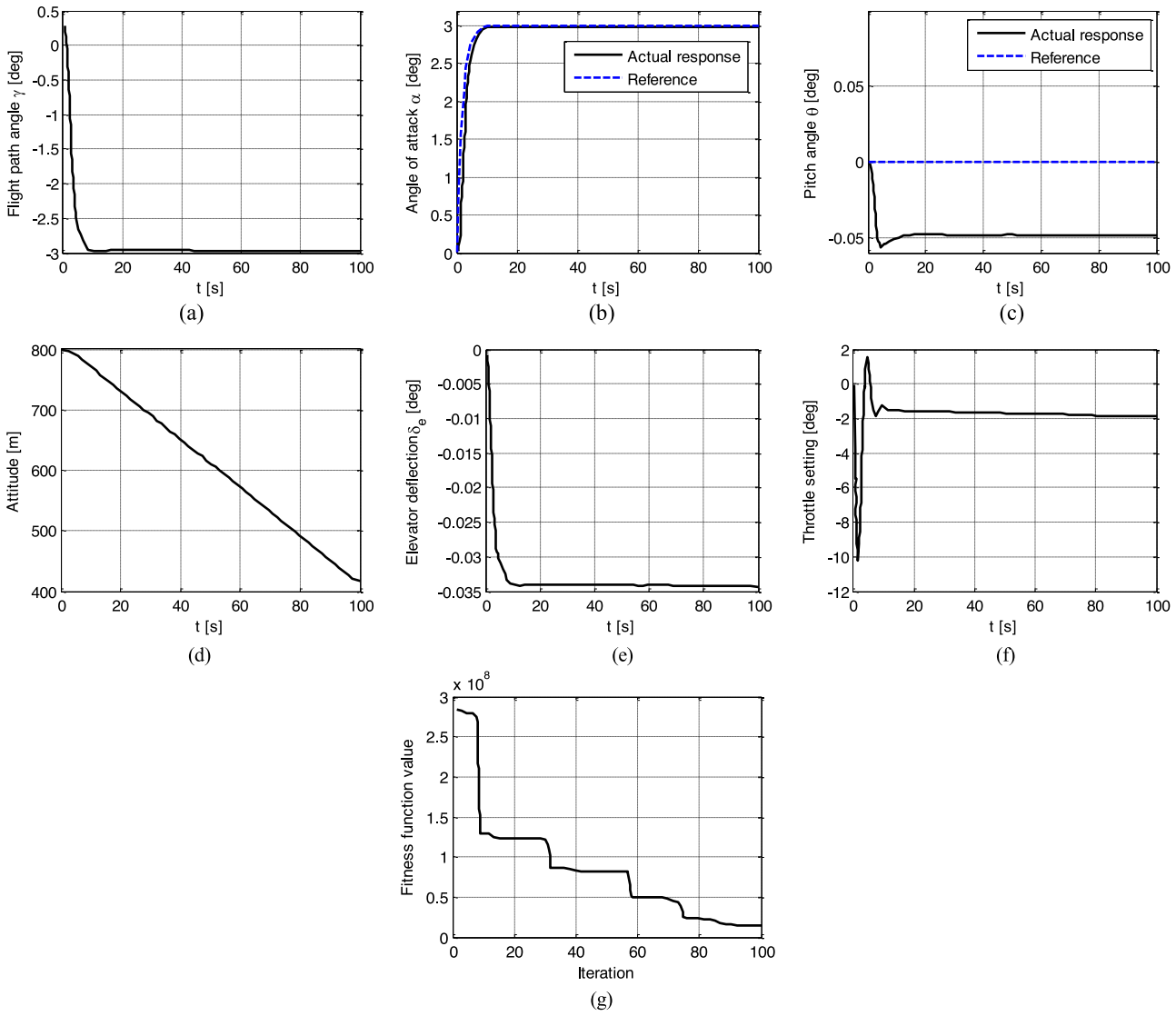

Fig. 8. Flight path angle tracking performance by AOA referenced APC in no-wind condition. (a) Flight path angle response. (b) Attack angle response. (c) Pitch angle response. (d) Altitude response. (e) Elevator deflection. (f) Throttle setting. (g) Evolution curve of PPPIO for AOA referenced ALS optimization.

IV. SIMULATION RESULTS

In this section, various examples are used to test the feasibility and optimality of the proposed ALS. The proposed longitudinal autopilot and APC are illustrated using a fix-wing UAV model. Two types of APCs are adopted to achieve flight path angle tracking. The feasibility and effectiveness of the PPPIO approach for ALS control parameter tuning are also investigated.

The following examples examine whether the controls given by the proposed ALS can meet the requirement, and whether the UAV can follow the desired flight path angle when using APCs. In the first example, the airspeed referenced APC is used, while the AOA referenced APC is employed in the second example. Therefore, the control parameter vectors to be decided are different in different examples.

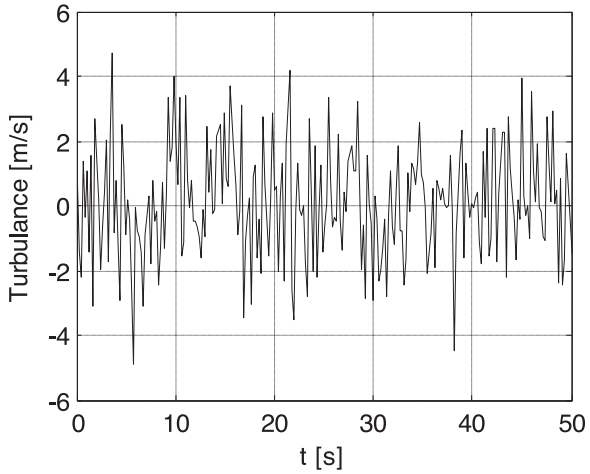

Fig. 9. Example of wind disturbances.

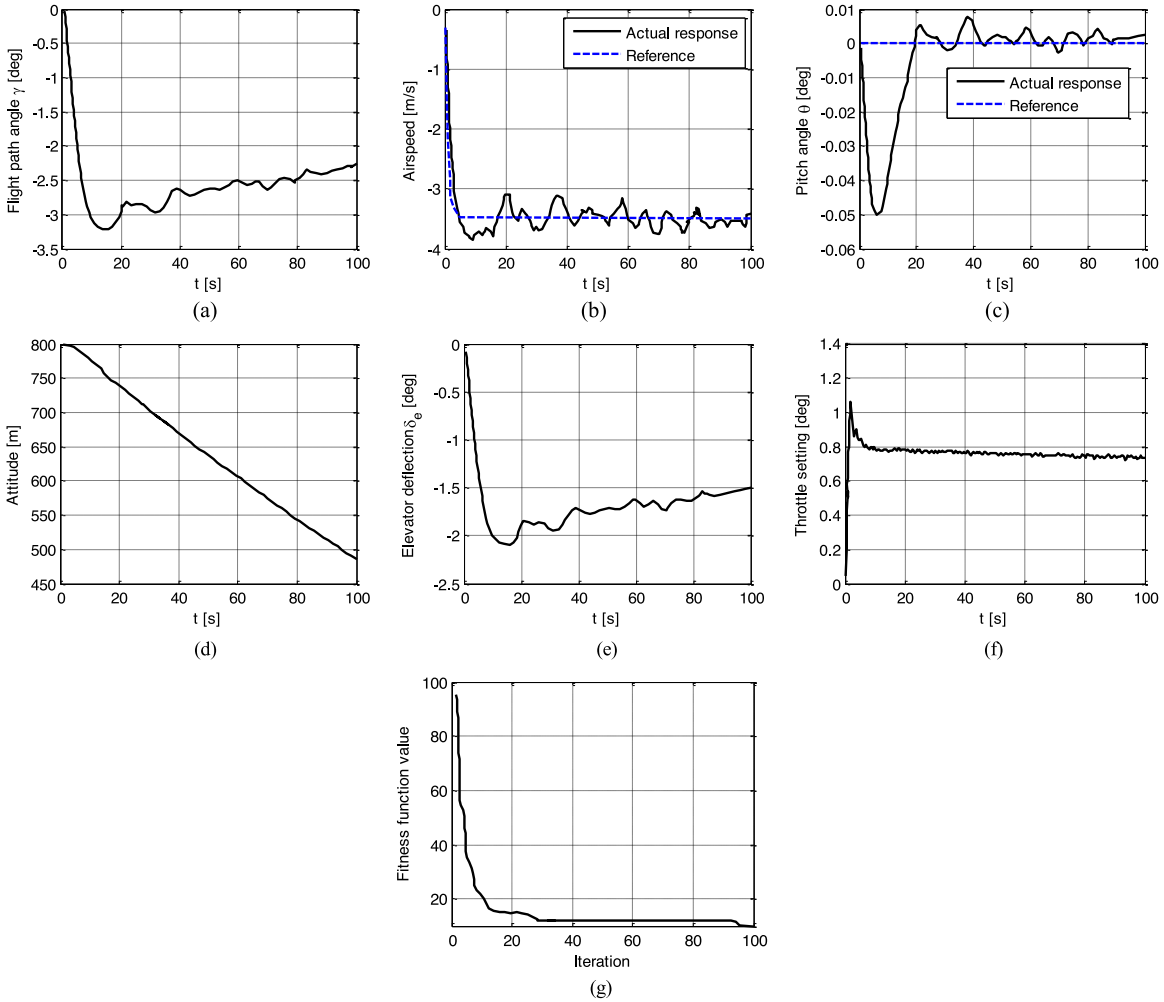

Fig. 10. Flight path angle tracking performance by achieved by airspeed referenced APC with wind disturbances. (a) Flight path angle response. (b) Airspeed response. (c) Pitch angle response. (d) Altitude response. (e) Elevator deflection. (f) Throttle setting. (g) Evolution curve of PPPIO for airspeed referenced ALS optimization with wind disturbances.

Although the actuator dynamics are fast enough and do not significantly alter the effect of the controller, they are considered in the UAV model. The actuator dynamics are added after the UAV dynamics described previously. The low-order approximations for the actuator are given by

$$\frac{\delta_e}{\delta_{\text{ec}}} = \frac{1325}{s^2 + 29.85s + 1325}. \tag{27}$$

When we augmented the actuator dynamics to the control system, there is not a significant change in the response. However, the engine dynamics are quite slow, and the adequacy of the ALS including the engine dynamics should be verified. The APC servo and the engine dynamics [4] are given by the following:

$$\frac{\delta_{\text{PL}}}{\delta_{\text{PLc}}} = \frac{1100}{s^2 + 33.17s + 1100} \tag{28}$$

$$\frac{\delta_T}{\delta_{\text{PL}}} = \frac{2.994(s^3 + 3.5s^2 + 9.18s + 3.13)}{s^4 + 6.5s^3 + 18.25s^2 + 26.28s + 9.37}. \tag{29}$$

The control signals are submitted to rate limits and saturations [36] as

$$-25\frac{\pi}{180}\,\text{rad} \le \delta_e \le 30\frac{\pi}{180}\text{rad} \tag{30}$$

$$-15\frac{\pi}{180}\text{rad/s} \le \dot{\delta}_e \le 15\frac{\pi}{180}\text{rad/s} \tag{31}$$

$$0.5\frac{\pi}{180}\text{rad} \le \delta_{\text{PL}} \le 10\frac{\pi}{180}\text{rad} \tag{32}$$

$$-1.6\frac{\pi}{180}\text{rad/s} \le \dot{\delta}_{\text{PL}} \le 1.6\frac{\pi}{180}\text{rad/s}. \tag{33}$$

Suppose that the UAV starts the initial states of the automatic landing as follows. The flight height is 800 m, the desired flight path angle is –3°, and the airspeed of the UAV is $V_0 = 69.97$ m/s. The desired value of airspeed is 66.5 m/s. The initial vertical rate, pitch angle, and attack angle of the UAV are set as zeros, and the referenced values are 0, 0°, and 3°, respectively. The flight path angle, airspeed, vertical rate, pitch angle, and attack angle are expressed as incremental values in following simulation results.

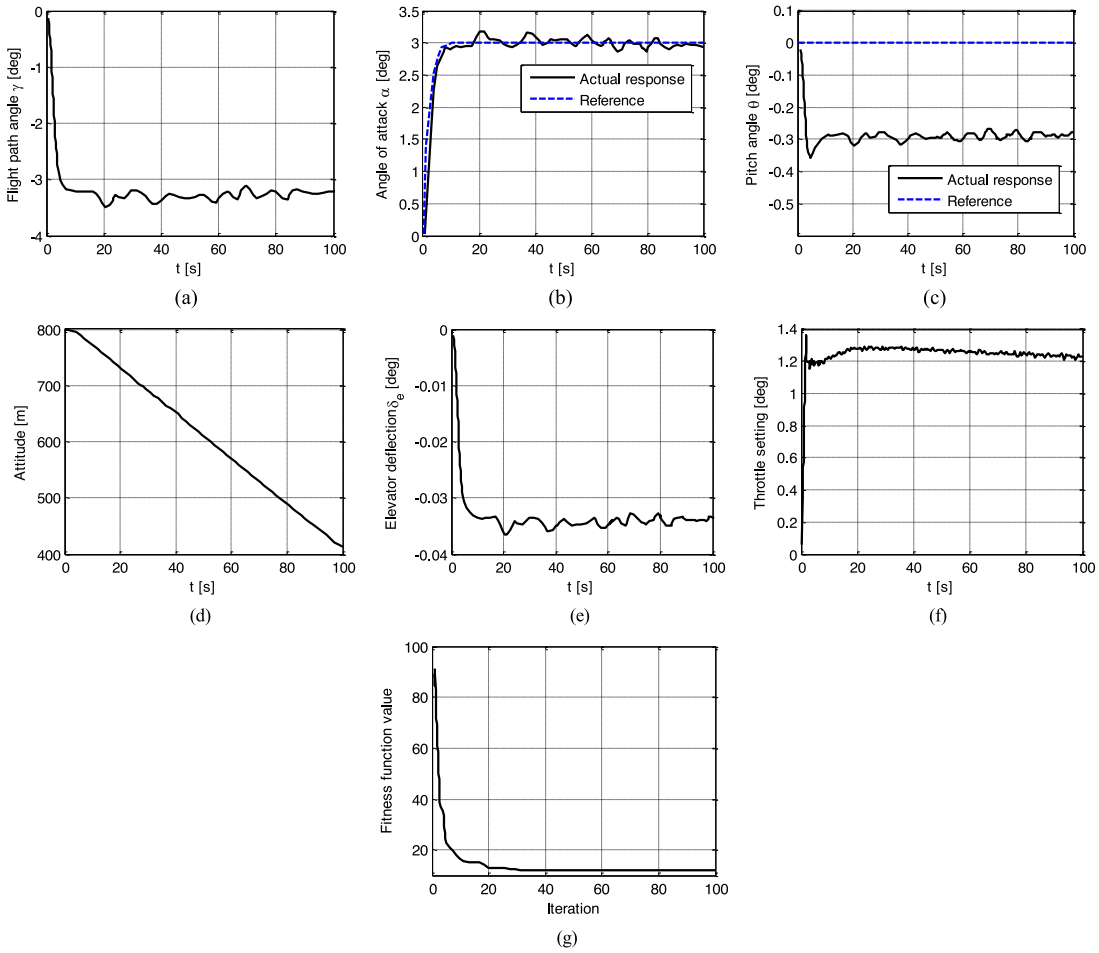

Fig. 11. Flight path angle tracking performance achieved by AOA referenced APC with wind disturbances. (a) Flight path angle response. (b) Attack angle response. (c) Pitch angle response. (d) Altitude response. (e) Elevator deflection. (f) Throttle setting. (g) Evolution curve of PPPIO for AOA referenced ALS optimization with wind disturbances.

Figs. 7 and 8 gave flight path angle tracking performances resulting from different ALSs corresponding to airspeed referenced APC and AOA referenced APC, respectively. Figs. 7(b) and (c), and 8(b) and (c) provide the difference between the actual responses and the reference signal, which are related to airspeed, attack angle, and pitch angle. It appears clearly that the path angle tracking can be achieved under the control of both the two types of APCs. While AOA referenced APC provides better results, the flight path angle converges toward the desired value and keeps stable.

Fig. 7(g) describes the relationship of the objective function and iteration count of PPPIO and six other algorithms, including the biogeography-based optimization, differential evolution algorithm, GA, stud genetic algorithm, and PIO. The value of the objective function represents the integral of the error between the pitch angle, airspeed or AOA actual outputs, and referenced signals. The smaller the integral value is, the better the ALS performs. From Fig. 7(g), we can conclude that the PPPIO performs the best among all the other six algorithms. Figs. 8(g), 10(g), and 11(g) illustrate the evolution curves of PPPIO for ALS optimization. The results are presented for 200 particles in 100 iterations. The evolution curves show the cost function's trend over iterations, representing that the particles reach the approximate optimum point in the feasible area.

The influence of wind disturbances on UAV are reflected as complex nonlinear functions of UAV states, including Mach number, altitude, rotation rates, AOA, control surfaces, thrust changes, and flap setting [37]. The stochastic wind components are based on the Dryden spectrum model with normalized white Gaussian noise, which can be considered as sets of linear filters. The longitudinal wind disturbance presented here according to [38] can be expressed as

$$H_{\delta x}(s) = \sigma_x \sqrt{\frac{2L_{xx}}{V_a}} \frac{1}{1 + (L_{xx}/V_a)s} \tag{34}$$

$$H_{\delta z}(s) = \sigma_z \sqrt{\frac{L_{zz}}{V_a}} \frac{1 + \sqrt{3}(L_{zz}/V_a)s}{[1 + (L_{zz}/V_a)s]^2} \tag{35}$$

where L_{xx} and L_{zz} denote the shape parameters related to the turbulence lengths, σ_x and σ_z represent the standard

deviations of independent processes, these parameters can be given by

$$\sigma_z = 0.1\ W_0 \tag{36}$$

$$\begin{cases} L_{xx} = L_{zz} = 305 \text{ m} \\ \sigma_x = \sigma_z \end{cases} z > 305 \text{ m} \tag{37}$$

$$\begin{cases} L_{\text{xx}} = \frac{z}{(0.177+0.0027z)^{1.2}} \\ L_{\text{zz}} = z \\ \sigma_x = \frac{\sigma_z}{(0.177+0.0027z)^{0.4}} \end{cases} z \leq 305 \text{ m} \tag{38}$$

where W_0 is the horizontal wind speed at 20 ft above the ground level.

In this study, the online estimation of the wind disturbances is also considered. The wind estimator is set up as a first-order filter with a time constant 0.35 s. To evaluate the efficiency of the ALS in the presence of wind disturbances, a wind turbulence provided by a Gauss white noise generator has been considered. Such wind is shown in Fig. 9. This wind turbulence is combined with the Dryden model mentioned above.

Figs. 10 and 11 display the flight path angle performances in the presence of wind when the main feedback signals airspeed and AOA are filled with noise. It is obvious that the UAV experienced less perturbation by using the control gains generated by AOA referenced APC. It appears that the proposed ALS keeps its performance, and the AOA referenced APC still provides faster and more stable flight path angle response. Figs. 10(g) and 11(g) display the evolution curves of PPPIO when optimizing the ALS under the condition of wind disturbances.

V. CONCLUSION

In this paper, a longitudinal ALS was presented to achieve flight path angle tracking during the approach of UAV. The main objective was to improve the tracking performance of the UAV along the longitudinal trajectory. The longitudinal UAV model was formulated. A pitch command longitudinal autopilot and two types of APCs were designed to achieve flight path angle tracking. The classic feedback technique was adopted in the ALS design. Furthermore, the ALS control parameter tuning was converted to a finite-dimensional optimization problem, which can be solved by the novel PPPIO. Several experimental results were presented, and the results showed that the tracking performance obtained from the proposed ALS was effective, and the proposed optimization technique was a feasible and efficient method for solving the ALS optimization problem. This approach helped solve control system optimization problems for different criteria and attains a rather accurate result. The major limitations of the proposed approach mainly hinged on simplifying modeling assumptions imposed on the problem. In particular, the influence of winds could have a significant impact on the solutions. A much more realistic model of the UAV and more complex fitness function in the optimization algorithm that account for different types of external disturbances are expected to improve the flight path tracking performance.

Our follow-up research will focus on extending the proposed bio-inspired intelligent algorithm such that it can be applied in handling other automatic mission problems of an unmanned system. In addition, it would be also worthwhile to use the proposed algorithm for other applications, such as the target searching problem and task planning problem.

REFERENCES

[1] M. Senpheng and M. Ruchanurucks
Automatic landing assistant system based on stripe lines on runway using computer vision
In *Proc. Int. Conf. Sci. Technol.*, 2015, pp. 35–39.

[2] P. Y. Guo, X. Li, and Y. Gui
Airborne vision-aided landing navigation system for fixed-wing UAV
In *Proc. IEEE 12th Int. Conf. Signal Process.*, 2014, pp. 1215–1220.

[3] A. Juliano and P. Ulisses
Automatic landing of a UAV using model predictive control for the surveillance of internal autopilot's controls
In *Proc. Int. Conf. Unmanned Aircr. Syst.*, 2014, pp. 1219–1224.

[4] M. B. Subrahmanyam
H∞ design of F/A-18A automatic carrier landing system
J. Guid., Control, Dyn., vol. 17, no. 1, pp. 187–191, 1994.

[5] Y. Li, N. Sundararajan, P. Saratchandran, and Z. F. Wang
Robust neuro-H∞ controller design for aircraft auto-landing
IEEE Trans. Aerosp. Electron. Syst., vol. 40, no. 1, pp. 158–167, Jan. 2004.

[6] M. Boulekchour, N. Aouf, and M. Richardson
Robust L∞ convex pose-graph optimisation for monocular localisation solution for unmanned aerial vehicles
Proc. Inst. Mech. Eng., Part G, J. Aerosp. Eng., vol. 229, no. 10, pp. 1903–1918, 2015.

[7] G. Looye, H. D. Joos, and R. F. Moomaw
Design of autoland controller functions with multiobjective optimization
J. Guid., Control, Dyn., vol. 29, no. 2, pp. 475–484, 2006.

[8] M. E. Kugler and F. Holzapfel
Autoland for a novel UAV as a state-machine-based extension to a modular automatic flight guidance and control system
In *Proc. Amer. Control Conf.*, 2017, pp. 2231–2236.

[9] J. F. Zhang and C. Jia
Automatic landing controller design and simulation of flying-wing unmanned aerial vehicle
In *Proc. 2nd Int. Conf. Meas., Inf. Control*, Harbin, China, 2013, pp. 893–896.

[10] R. Lungu and M. Lungu
Automatic landing control using H-inf control and dynamic inversion
Proc. Inst. Mech. Eng., Part G, J. Aerosp. Eng., vol. 228, no. 14, pp. 2612–2626, 2014.

[11] J. Karelahti, K. Virtanen, and J. Öström
Automated generation of realistic near-optimal aircraft trajectories
J. Guid., Control, Dyn., vol. 31, no. 3, pp. 674–688, 2008.

[12] K. Graichen and N. Petit
Constructive methods for initialization and handling mixed state-input constraints in optimal control
J. Guid., Control, Dyn., vol. 31, no. 5, pp. 1334–1343, 2008.

[13] K. Pontani and B. A. Conway
Particle swarm optimization applied to space trajectories
J. Guid., Control, Dyn., vol. 33, no. 5, pp. 1429–1441, 2010.

[14] Y. H. Shi and R. C. Eberhart
A modified particle swarm optimizer
In *Proc. IEEE Conf. Evol. Comput.*, Anchorage, AK, USA, 1998, pp. 69–73.

[15] H. B. Duan and P. X. Qiao
Pigeon-inspired optimization: A new swarm intelligence optimizer for air robot path planning
Int. J. Intell. Comput. Cybern., vol. 7, no. 1, pp. 24–37, 2014.

[16] H. B. Duan and X. H. Wang
Echo state networks with orthogonal pigeon-inspired optimization for image restoration
IEEE Trans. Neural Netw. Learn. Syst., vol. 27, no. 11, pp. 2413–2425, Nov. 2016.

[17] J. Kennedy and R. Eberhart
Particle swarm optimization
In *Proc. IEEE Int. Conf. Neural Netw.*, 1995, pp. 1942–1948.

[18] M. Dorigo, V. Maniezzo, and A. Colorni
Ant system: Optimization by a colony of cooperating agents
IEEE Trans. Syst. Man, Cybern. B, Cybern., vol. 26, no. 1, pp. 29–41, Feb. 1996.

[19] R. Dou and H. B. Duan
Pigeon inspired optimization approach to model prediction control for unmanned air vehicles
Aircr. Eng. Aerosp. Technol., vol. 88, no. 1, pp. 108–116, 2016.

[20] X. Chen and R. K. Agarwal
Shape optimization of airfoils in transonic flow using a multi-objective genetic algorithm
Proc. Inst. Mech. Eng., Part G, J. Aerosp. Eng., vol. 228, no. 9, pp. 1654–1667, 2014.

[21] H. B. Duan, Y. X. Yu, and Z. Y. Zhao
Parameters identification of UCAV flight control system based on predator-prey particle swarm optimization
Sci. China Inf. Sci., vol. 56, no. 1, pp. 1–12, 2013.

[22] P. J. Werbos
Computational intelligence for the smart grid-history, challenges, and opportunities
IEEE Comput. Intell. Mag., vol. 6, no. 3, pp. 14–21, Aug. 2011.

[23] C. Y. Li, W. X. Jing, and C. S. Gao
Adaptive backstepping-based flight control system using integral filters
Aerosp. Sci. Technol., vol. 13, no. 2, pp. 105–113, 2009.

[24] Y. Meng, Y. Y. Zhang, and Y. C. Jin
Autonomous self-reconfiguration of modular robots by evolving a hierarchical mechanochemical model
IEEE Comput. Intell. Mag., vol. 6, no. 1, pp. 43–54, Feb. 2011.

[25] R. Q. Chai, A. Savvaris, and A. Tsourdos
Trajectory optimization of space maneuver vehicle using a hybrid optimal control solver *IEEE Trans. Cybern.*,
pp. 1–14, doi: 10.1109/TCYB.2017.2778195.

[26] H. Yang, X. Bai, and H. Baoyin
Rapid generation of time-optimal trajectories for asteroid landing via convex optimization
J. Guid., Control, Dyn., vol. 40, no. 3, pp. 628–641, 2017.

[27] R. Chai, A. Savvaris, and A. Tsourdos
Improved gradient-based algorithm for solving aeroassisted vehicle trajectory optimization problems
J. Guid., Control, Dyn., vol. 40, no. 8, pp. 2093–2101, 2017.

[28] B. Zhang and H. B. Duan
Three-dimensional path planning for uninhabited combat aerial vehicle based on predator-prey pigeon-inspired optimization in dynamic environment
IEEE/ACM Trans. Comput. Biol. Bioinf., vol. 14, no. 1, pp. 97–107, Jan./Feb. 2017.

[29] H. Bouadi, F. Camino, and D. Choukroun
Space-indexed control for aircraft vertical guidance with time constraint
J. Guid., Control, Dyn., vol. 37, no. 4, pp. 1103–1113, 2014.

[30] J. M. Urnes and R. K. Hess
Development of the F/A-18A automatic carrier landing system
J. Guid., Control, Dyn., vol. 8, no. 3, pp. 289–295, 1985.

[31] K. Nho and R. K. Agarwal
Automatic landing system design using fuzzy logic
J. Guid., Control, Dyn., vol. 23, no. 2, pp. 298–304, 2000.

[32] R. W. Huff and G. K. Kessler
Enhanced displays, flight controls, and guidance systems for approach and landing
AGARD, Aircr. Ship Oper., pp. 97–104, 1991.

[33] H. X. Qiu and H. B. Duan
Multi-objective pigeon-inspired optimization for brushless direct current motor parameter design
Sci. China Technol. Sci., vol. 58, no. 11, pp. 1915–1923, 2015.

[34] H. B. Duan and H. X. Qiu
Unmanned Aerial Vehicles Swarm Autonomous Control Based on Swarm Intelligence. Science Press, Beijing, China, 2018.

[35] D. F. Zhang and H. B. Duan
Identification for a reentry vehicle via Levy flight-based pigeon-inspired optimization
Proc. Inst. Mech. Eng. Part G, J. Aerosp. Eng., vol. 232, no. 4, pp. 626–637, 2018.

[36] A. Chakraborty, P. Seiler, and G. J. Balas
Susceptibility of F/A-18 flight controllers to the falling-leaf mode: Linear analysis
J. Guid., Control, Dyn., vol. 34, no. 1, pp. 57–72, 2011.

[37] Y. M. Deng and H. B. Duan
Control parameter design for automatic carrier landing system via pigeon-inspired optimization
Nonlinear Dyn., vol. 85, no. 1, pp. 97–106, 2016.

[38] C. W. Campbell
A spatial model of wind shear and turbulence for flight simulation
NASA, Washington, DC, USA, NASA Tech. Rep. TR-TP-2313, 1984.

Haibin Duan (M'07–SM'08) received the college degree in mechanical engineering from Xi'an Aeronautical University in 1996, and the Ph.D. degree in control theory and control engineering from Nanjing University of Aeronautics and Astronautics(NUAA) in 2005. He is a Full Professor with the School of Automation Science and Electrical Engineering, Beihang University, Beijing, China. He is the Vice Director of the State Key Laboratory of Virtual Reality Technology and Systems, and is also the head of the Bio-inspired Autonomous Flight Systems (BAFS) Research Group, Beihang University. He received the National Science Fund for Distinguished Young Scholars of China. He is also enrolled in the Scientific and Technological Innovation Leading Talent of "Ten Thousand Plan"-National High Level Talents Special Support Plan, Top-Notch Young Talents Program of China, Program for New Century Excellent Talents in University of China, and Beijing NOVA Program. He has authored or coauthored more than 70 publications and three monographs. His current research interests are bio-inspired computing, biological computer vision, and multi-UAV autonomous formation control.

Mengzhen Huo received the B.S. degree in automation science from Beihang University, Beijing, China, in 2018. She is currently working toward the Ph.D. degree with the BAFS Research Group, State Key Laboratory of Virtual Reality Technology and Systems, School of Automation Science and Electrical Engineering, Beihang University.

Her current research interests include bio-inspired computation and unmanned aerial vehicle cooperative control.

Zhiyuan Yang received the B.S. degree in automation from Beihang University, Beijing, China, in 2016. He is currently working toward the master's degree with the State Key Laboratory of Virtual Reality Technology and Systems, School of Automation Science and Electrical Engineering, Beihang University.

His research interests include bio-inspired computation and flight control.

Yuhui Shi (M'96–SM'98–F'16) received the bachelor degree in electrical engineering from Hunan University in 1984, master degree in biomedical engineering from Chongqing University in 1988, Ph.D. degree in signal processing from Southeast University in 1992. He is a Chair Professor with the Department of Computer Science and Engineering, Southern University of Science and Technology (SUSTech), Shenzhen, China. Before joining SUSTech, he was with the Department of Electrical and Electronic Engineering, Xi'an Jiaotong-Liverpool University (XJTLU), Suzhou, China, from January 2008 to August 2017, was with the Electronic Data Systems Corporation (EDS), IN, USA, from October 1998 to December 2007, and was with the Purdue School of Engineering and Technology, IN, USA, from October 1995 to September 1998. He is the Editor-in-Chief of the *International Journal of Swarm Intelligence Research* and an Associate Editor of the IEEE TRANSACTIONS ON EVOLUTIONARY COMPUTATION. His research interests include swarm intelligence and applications.

Qinan Luo received the B.Sc. degree in automation science from Beihang University, Beijing, China, in 2011. He is currently working toward the Ph.D. degree with the School of Automation Science and Electrical Engineering, Beihang University.

His current research interests include advanced flight control, bio-inspired computing, and intelligent information processing.